



Effect of Mn^{2+} -doping in LiFePO_4 and the low temperature electrochemical performances

Chengfeng Li^{a,b,c}, Ning Hua^{a,b,c}, Chengyun Wang^{a,b,c}, Xueya Kang^{a,c,*},
Tuerdi Wumair^{a,c}, Ying Han^{a,c}

^a Xinjiang Technical Institute of Physics and Chemistry, Chinese Academy of Sciences, Urumqi Xinjiang 830011, China

^b Graduate University of Chinese Academy of Sciences, Beijing 100049, China

^c Xinjiang Key Laboratory of Electronic Information Materials and Devices, Urumqi Xinjiang 830011, China

ARTICLE INFO

Article history:

Received 21 June 2010

Received in revised form 20 October 2010

Accepted 21 October 2010

Available online 29 October 2010

Keywords:

Olivine compound

Electrochemical performance

Low temperature performance

Chelation assisted method

Mn^{2+} -doping

ABSTRACT

Olivine composites $\text{LiFe}_{1-x}\text{Mn}_x\text{PO}_4/\text{C}$ ($x = 0, 0.05, 0.1$) were prepared by chelation assisted mechanochemical activation method using $\text{C}_2\text{H}_2\text{O}_4$ as the chelating reagent. The structures of the prepared composites were characterized by X-ray diffraction (XRD). Cyclic voltammetry, ac impedance spectroscopy, galvanostatic charge/discharge performances were studied at room temperature. The discharge capacity of $\text{LiFe}_{0.95}\text{Mn}_{0.05}\text{PO}_4$ was 155.6 mAh g^{-1} and 102.9 mAh g^{-1} at 1 C and 10 C rate, respectively. The results indicated Mn^{2+} -doping in LiFePO_4 could effectively enhance the electrochemical performances of this olivine compound especially at high charge/discharge rate. In addition, charge/discharge method was also used to characterize the low temperature properties of the different samples. The results showed that the lower the operation temperature was, the poorer the performances were. Furthermore, ac impedance measurement was used to understand the factors of the poor performances at low temperature.

© 2010 Elsevier B.V. All rights reserved.

1. Introduction

Since the work of Goodenough and co-workers [1,2], olivine structured LiFePO_4 has been investigated intensively as cathode materials for lithium batteries because of their high stabilities, environmental benign and high theoretical capacities (170 mAh g^{-1}) [3–5]. However, their intrinsic low electronic conductivity [3] and poor ionic transport property [6] have largely hindered the development of this cathode material. For these reasons, few works about these materials had been reported till the landmark work finished by Chung et al. [3], whom enhanced the electronic conductivity with a factor of $\sim 10^8$ by aliovalent doping. Till now, based on the numerous work about these olivine compounds, several concepts have been concluded to increase their electrochemical performances [7,8], such as (i) decreasing the particle size to lessen the diffusion distance and increase the surface area by advanced synthesis techniques [9], (ii) increasing the electronic conductivity by surface coating with conductive carbon or other electronic conducting metal or oxide [10–13], (iii) selective doping with supervalent cations to increase the intrinsic electronic con-

ductivity [14]. In the olivine family, LiMnPO_4 was also an attractive cathode material for its high potential of 4.1 V vs. Li^+/Li [15]. But its poor electrochemical performances limited its practical usage. However, Mn^{2+} -doping in $\text{LiFe}_{1-x}\text{Mn}_x\text{PO}_4$ solid solution could significantly improve the kinetic properties of LiFePO_4 in the region of $0 \leq x \leq 0.75$ [16–18]. So it might be an effective way to enhance the electrochemical performances of LiFePO_4 . In this work, we have successfully prepared Mn^{2+} doped $\text{LiFe}_{1-x}\text{Mn}_x\text{PO}_4$ composites by chelation assisted mechanochemical activation method using $\text{C}_2\text{H}_2\text{O}_4$ as the chelating reagent and using water as the media of ball-mill procedure. These Mn^{2+} -doping composites showed an enhancement of high rate capacities and cycling stabilities.

Further considering the practical usage of LiFePO_4 , a very important aspect was the low temperature performances. Several reports had already been published about the low temperature performances of this material [19,21]. We also attempted to enhance the low temperature performances by Mn^{2+} -doping. But the results indicated that there was little improvement which indicated other method should be used to solve this problem. Ac impedance spectroscopy was also used to investigate the low temperature properties of Mn^{2+} -doping samples. From the results we could get that the R_{ct} (correspond to charge transfer resistance) increased largely while decreasing the operation temperature, which indicated electrolyte optimization and surface modification might be the most effective way to enhance the low temperature performances.

* Corresponding author at: Xinjiang Technical Institute of Physics and Chemistry, Chinese Academy of Sciences, Urumqi Xinjiang 830011, China.
Tel.: +86 991 3850517; fax: +86 991 3850517.

E-mail address: xueyakang@yahoo.cn (X. Kang).

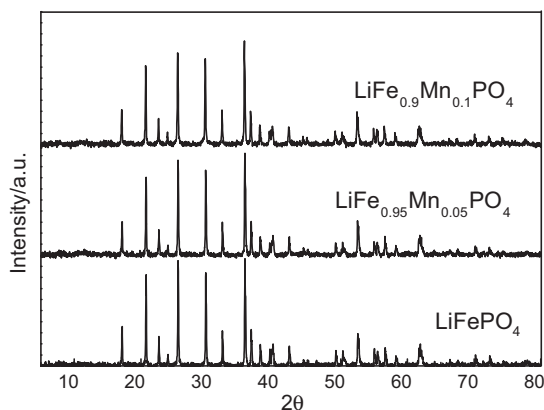


Fig. 1. XRD patterns of the synthesized $\text{LiFe}_{1-x}\text{Mn}_x\text{PO}_4$ ($x = 0, 0.05, 0.1$).

2. Experimental

2.1. Sample preparation

$\text{LiFe}_{1-x}\text{Mn}_x\text{PO}_4$ composites were prepared by chelation assisted mechanochemical activation method using $\text{C}_2\text{H}_2\text{O}_4$ as the chelating reagent. Stoichiometric amount of $\text{NH}_4\text{H}_2\text{PO}_4$, $\text{Mn}(\text{CH}_3\text{COO})_2 \cdot 4\text{H}_2\text{O}$, $\text{FePO}_4 \cdot 2\text{H}_2\text{O}$ and $\text{LiOH} \cdot \text{H}_2\text{O}$ were ball milled with 15 wt.% $\text{C}_2\text{H}_2\text{O}_4$ for 7 h using deionised-water as the media of ball-milling. Polyurethane vessel and ZrO_2 balls were used during ball-milling procedure (QM-3SP4, Nanjing NanDa Instrument Plant) with a ball-to-powder ratio (weight ratio) of 4:1 and a rotation speed of 350 rpm. The milled powder was dried at 70°C in a dry oven. After the powder was dried, 15 wt.% glucose was added while grinding the powder in mortar. Then the powder was sintered in a tube furnace at 700°C for 10 h using nitrogen atmosphere to avoid the oxidation of Fe^{2+} .

2.2. Sample characterization

The phase structure of the obtained samples were investigated by X-ray diffraction (XRD, RINT-2500 V, Rigaku Co.) using $\text{Cu K}\alpha$ radiation ($\lambda = 1.5418 \text{ \AA}$) in the range of $5\text{--}80^\circ$ with a scanning rate of 2° per min. To test the electrochemical performances, the cathode was prepared by spreading the cathode slurry (80 wt.% of the active material) onto an aluminum foil followed by drying in vacuum at 120°C for 12 h. The cells (CR2025) were assembled in an argon filled glove-box using lithium metal foil as the counter electrode. The electrolyte was 1.0 mol dm^{-3} LiPF_6 in a mixture of ethyl carbonate (EC), diethyl carbonate (DEC) and dimethyl carbonate (DMC) (volume ratio 1:1:1). Electrochemical performances of LiFePO_4 were investigated by using CR2025 coin-type cell. The cells were charged and discharged between 2.3 V and 4.3 V on a charge/discharge apparatus (BTS-51, Neware, China). Cyclic voltammetry (CV) and electrochemical impedance spectroscopy (EIS) were conducted by using a CHI650 electrochemical working station. The sinusoidal excitation voltage of EIS was 10 mV and the frequency range was between 10^5 and 10^{-2} Hz.

3. Results and discussion

All the samples were successfully synthesized by this chelation assisted method which could be verified by the XRD patterns

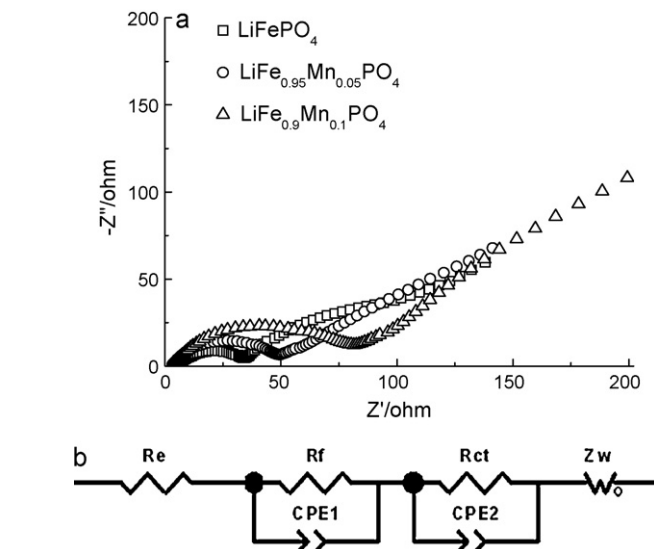
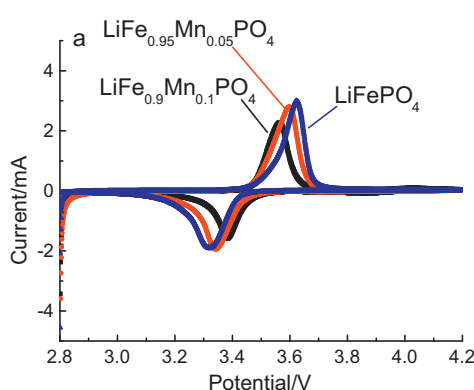


Fig. 3. (a) Nyquist plots of the three composites. (b) Equivalent circuit model used for EIS fitting of the electrode.

(Fig. 1). All the peaks could be indexed as orthorhombic structure belonging to the space group $Pnma$ (JCPDS No. 40-1499). The absence of any other signals indicated there were no high content impurities related to Mn^{2+} or Fe^{3+} compounds and the residual carbon decomposed from glucose was amorphous in these composites. The results illustrated the feasibility of our method for the preparation of $\text{LiFe}_{1-x}\text{Mn}_x\text{PO}_4$.

To evaluate the effect of Mn^{2+} substitution, cyclic voltammetry was used at room temperature. Fig. 2 was the profiles of the prepared samples. From Fig. 2(a) a more symmetric curve with smaller interval between the cathodic and anodic peak current was obtained by Mn^{2+} substitution. This denoted a decreasing of polarization with Mn^{2+} substitution, which illustrated an enhancement of electrochemical performances. Fig. 2(b) showed the CV curves of $\text{LiFe}_{0.95}\text{Mn}_{0.05}\text{PO}_4$ at the sweeping rate of 0.1 mV s^{-1} , 0.2 mV s^{-1} , 0.5 mV s^{-1} and 1 mV s^{-1} , respectively. It could be seen in Fig. 2(b), as the sweeping rate was raised the oxidation peak shifted higher and the reduction peak sifted lower. And the reduction peaks in Fig. 2(a) and (b) seemed more vulnerable to the variety of Mn^{2+} content and sweeping rate which was coincidence with the work of Nakamura et al. [16].

The electrode impedance of these prepared composites was also evaluated at room temperature. Fig. 3(a) presented the Nyquist plots of the composites at the same charge/discharge state. The impedance spectra were fitted with the fitting equivalent circuit as

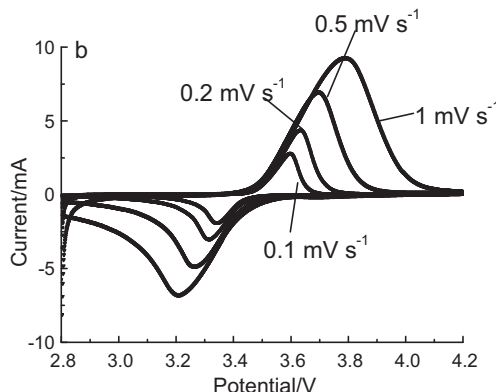


Fig. 2. (a) CV curves of the composites at 0.1 mV s^{-1} . (b) CV profiles of $\text{LiFe}_{0.95}\text{Mn}_{0.05}\text{PO}_4$ at different sweeping rate.

Table 1
Impedance parameters of $\text{LiFe}_{1-x}\text{Mn}_x\text{PO}_4$ fitted with equivalent circuit.

| | R_e/Ω | R_f/Ω | R_{ct}/Ω |
|---|--------------|--------------|-----------------|
| LiFePO_4 | 5.283 | 7.184 | 21.11 |
| $\text{LiFe}_{0.95}\text{Mn}_{0.05}\text{PO}_4$ | 3.273 | 8.484 | 34.55 |
| $\text{LiFe}_{0.9}\text{Mn}_{0.1}\text{PO}_4$ | 4.06 | 11.7 | 54.64 |

shown in Fig. 3(b). According to the literature [21], R_e represents the solution resistance, R_f signify the diffusion resistance of Li-ions through the solid electrolyte interface (SEI) layer, R_{ct} correspond to the charge transfer resistance. Z_w is related to the solid-state diffusion of Li-ions in the active materials corresponding to the slopping line at the low frequency. The fitting results were shown in Table 1. It was obviously that R_{ct} was increasing with the rising of the substitution content. This phenomenon illustrated that even if the enhanced electrochemical performances could be obtained by Mn^{2+} substitution, the surface charge transfer resistance represented by R_{ct} still increased. It is well known that LiMnPO_4 has very poor electrochemical performances when compared with LiFePO_4 , duo to its insulation property [15]. The increased R_{ct} might be ascribed to the existence of Mn^{2+} substituted olivine structure on the surface of the crystals, which hindered the charge transfer reaction on the surface.

The charge/discharge curves of $\text{LiFe}_{0.95}\text{Mn}_{0.05}\text{PO}_4$ at room temperature were exhibited in Fig. 4. As shown in Fig. 4, the discharge capacities of this composite were 160.8 mAh g^{-1} , 155.6 mAh g^{-1} , 146.6 mAh g^{-1} , 129.6 mAh g^{-1} and 102.9 mAh g^{-1} at 0.5 C, 1 C, 2 C, 5 C, 10 C rate, respectively. Fig. 5 showed the cycling profiles of the different composites at room temperature. At first, the capacity of

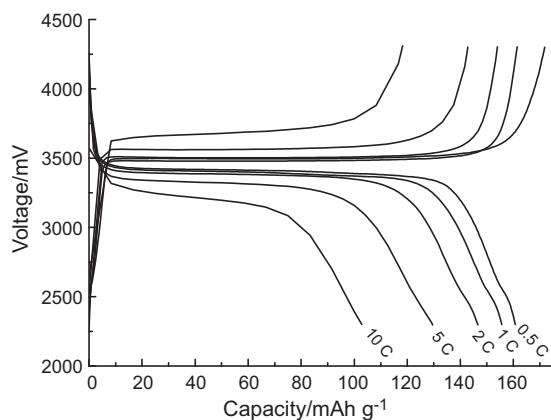


Fig. 4. Charge/discharge curves of $\text{LiFe}_{0.95}\text{Mn}_{0.05}\text{PO}_4$ at different C rates.

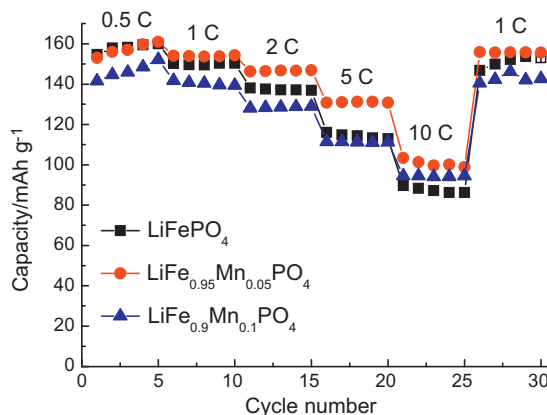


Fig. 5. Cycling profiles of the composites.

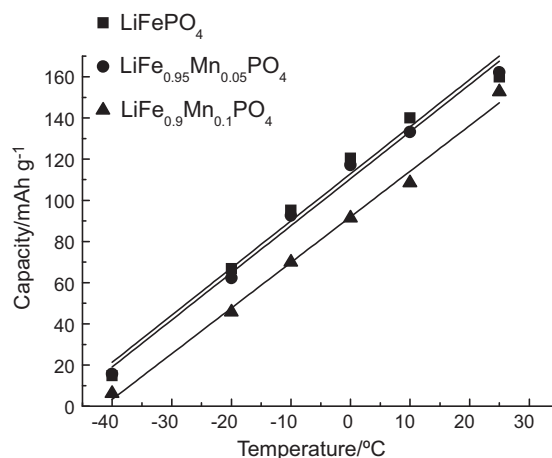


Fig. 6. Capacities of the composites at different temperatures.

the three composites was slightly increasing, which could be seen in many reports using CTR method [20]. While the raise of the C rate, the advantage of Mn^{2+} substitution became notable. Even the capacity of $\text{LiFe}_{0.9}\text{Mn}_{0.1}\text{PO}_4$ exceeded the non-substituted one at 10 C and stable at this capacity. So the electrochemical performances (especially the high rate performances) of olivine LiFePO_4 could be effectively enhanced by Mn^{2+} substitution, duo to the improved electronic conductivity and ionic transportation [16].

Further considering the practical usage of $\text{LiFe}_{1-x}\text{Mn}_x\text{PO}_4$, we investigated the low temperature performances of the prepared composites by galvanostatic charge/discharge method. The relationship of capacity to temperature was displayed in Fig. 6. While lowering the temperature, the capacities of the composites decreased largely. This phenomenon indicated a poor electrochemical performance at low temperature, which should be improved for the practical, large-scale usage of these composites. From Fig. 6, the capacity decreased linearly when lowering the temperature and the slopes were nearly the same, which were irrespective to such different composites. It was interesting that the kinetic enhanced properties almost had no impact on the low temperature performances. To answer this puzzle, ac impedance spectroscopy was used to investigate the impedance property of $\text{LiFe}_{0.95}\text{Mn}_{0.05}\text{PO}_4$ at low temperature. The Nyquist plots at different temperatures were presented in Fig. 7. It was obviously that the R_{ct} increased largely as the temperature decreased, especially when the temperature fell below -20°C . The spectra were also fitted with the equivalent circuit as shown in Fig. 3(b). The impedance parameters were listed in Table 2. From the table, the decreasing of temperature showed much pronounced influence on R_{ct} which represented charge trans-

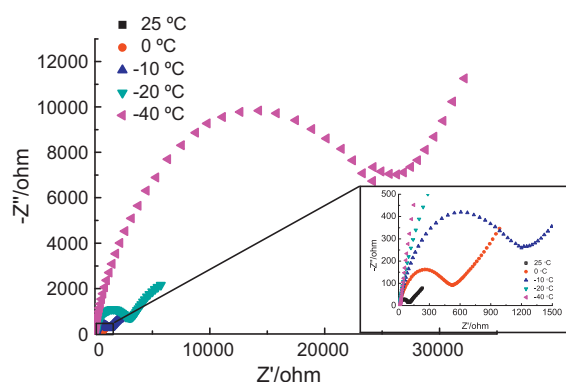


Fig. 7. Nyquist plots of $\text{LiFe}_{0.95}\text{Mn}_{0.05}\text{PO}_4$ at different temperature.

Table 2
Impedance parameters of $\text{LiFe}_{0.95}\text{Mn}_{0.05}\text{PO}_4$ at different temperatures.

| Temperature | R_e/Ω | R_f/Ω | R_{ct}/Ω |
|-------------|--------------|--------------|---------------------|
| 25 °C | 6.321 | 18.18 | 69.55 |
| 0 °C | 9.212 | 68.84 | 376.6 |
| −10 °C | 7.967 | 115.6 | 921.5 |
| −20 °C | 8.676 | 286.5 | 2233 |
| −40 °C | 10.94 | 2481 | 1.959×10^4 |

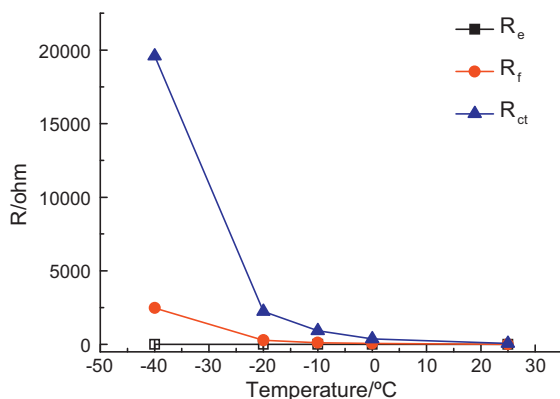


Fig. 8. Comparison for temperature dependency of the different resistances.

fer reaction occurring at the electrode/electrolyte interface (as shown in Fig. 8). These results indicated that Mn^{2+} substitution had few influences on the low temperature performances. The most effective way to enhance the low temperature performances might be decreasing the R_{ct} by facilitating the charge transfer reaction, which could be solved by surface modification or electrolyte optimization.

4. Conclusion

In this work, we introduced a chelation assisted mechanochemical activation method with $\text{C}_2\text{H}_2\text{O}_4$ as the chelating reagent to prepare $\text{LiFe}_{1-x}\text{Mn}_x\text{PO}_4$ composites. The structures of the composites were characterized by X-ray diffraction. The electrochemical properties at room temperature were investigated by galvanostatic charge/discharge method, cyclic voltammetry, ac impedance spectroscopy. The results showed that the electrochemical performances were enhanced by Mn^{2+} substitution, especially at high

charge/discharge rate. In addition, galvanostatic charge/discharge method was also used to characterize the low temperature properties of these composites. The results showed that the lower the operation temperature was, the poorer the performances were. Furthermore, ac impedance measurements were used to understand the factors of the poor performances at low temperature. From the results, the decreasing of temperature showed much pronounced influence on R_{ct} which represented charge transfer reaction occurring at the electrode/electrolyte interface. This indicated that the most effective way to enhance the low temperature performances might be decreasing the R_{ct} by facilitating the charge transfer reaction which could be solved by surface modification or electrolyte optimization.

References

- [1] A.K. Padhi, K.S. Nanjundaswamy, J.B. Goodenough, *J. Electrochem. Soc.* 144 (1997) 1188–1194.
- [2] A.K. Padhi, K.S. Nanjundaswamy, C. Masquelier, S. Okada, J.B. Goodenough, *J. Electrochem. Soc.* 144 (1997) 1609–1613.
- [3] S.Y. Chung, J.T. Bloking, Y.M. Chiang, *Nat. Mater.* 1 (2002) 123–128.
- [4] C. Delacourt, P. Poizot, J.M. Tarascon, C. Masquelier, *Nat. Mater.* 4 (2005) 254–260.
- [5] M. Thackeray, *Nat. Mater.* 1 (2002) 81–82.
- [6] B. Zhang, X.J. Wang, Z.J. Liu, H. Li, X.J. Huang, *J. Electrochem. Soc.* 157 (2010) A285–A288.
- [7] D. Zhang, X. Yu, Y.F. Wang, R. Cai, Z.P. Shao, X.Z. Liao, Z.F. Ma, *J. Electrochem. Soc.* 156 (2009) A802–A808.
- [8] F. Yu, J.J. Zhang, Y.F. Yang, G.Z. Song, *J. Mater. Chem.* 19 (2009) 9121–9125.
- [9] L. Wang, Y. Huang, R. Jiang, D. Jia, *Electrochim. Acta* 52 (2007) 6778–6783.
- [10] Y. Wang, Y. Wang, E. Hosono, K. Wang, H. Zhou, *Angew. Chem. Int. Ed.* 47 (2008) 7461–7465.
- [11] S. Yang, Y. Song, P.Y. Zavalij, M. Stanley Whittingham, *Electrochem. Commun.* 4 (2002) 239–244.
- [12] S.L. Bewlay, K. Konstantinov, G.X. Wang, S.X. Dou, H.K. Liu, *Mater. Lett.* 58 (2004) 1788–1791.
- [13] F. Croce, A.D. Epifanio, J. Hassoun, A. Deptula, T. Olczac, B. Scrosati, *Electrochem. Solid State* 5 (2002) A47–A50.
- [14] L.J. Li, X.H. Li, Z.X. Wang, L. Wu, J.C. Zheng, H.J. Guo, *J. Phys. Chem. Solids* 70 (2009) 238–242.
- [15] S.K. Martha, B. Markovsky, J. Grinblat, Y. Gofer, O. Haik, E. Zinigrad, D. Aurbach, T. Drezen, D. Wang, G. Deghenghi, I. Exnar, *J. Electrochem. Soc.* 156 (2009) A541–A552.
- [16] T. Nakamura, K. Sakamoto, M. Okamoto, S. Seki, Y. Kobayashi, T. Takeuchi, M. Tabuchi, Y. Yamada, *J. Power Sources* 174 (2007) 435–441.
- [17] A. Yamada, H. Koizumi, S.I. Nishimura, N. Sonoyama, R. Kanno, M. Yonemura, T. Nakamura, Y. Kobayashi, *Nat. Mater.* 5 (2006) 357–360.
- [18] A. Yamada, Y. Kudo, K.Y. Liu, *J. Electrochem. Soc.* 148 (2001) A747–A754.
- [19] X.Z. Liao, Z.F. Ma, Q. Gong, Y.S. He, L. Pei, L.J. Zeng, *Electrochem. Commun.* 10 (2008) 691–694.
- [20] H.P. Liu, Z.X. Wang, X.H. Li, H.J. Guo, W.J. Peng, Y.H. Zhang, Q.Y. Hu, *J. Power Sources* 184 (2008) 469–472.
- [21] S.S. Zhang, K. Xu, T.R. Jow, *J. Power Sources* 159 (2006) 702–707.